

Theoretical calculations of shallow acceptor states in GaAs/Al_xGa_{1-x}As quantum wells in the presence of an external magnetic field

Q. X. Zhao and P. O. Holtz

Department of Physics and Measurement Technology, Linköping University, S-581 83 Linköping, Sweden

Alfredo Pasquarello

Institut Romand de Recherche Numérique en Physique des Matériaux (IRRMA), PHB-Ecublens, CH-1015 Lausanne, Switzerland

B. Monemar and M. Willander

Department of Physics and Measurement Technology, Linköping University, S-581 83 Linköping, Sweden

(Received 24 February 1994)

Energy levels of ground and excited shallow acceptor states in the presence of an external magnetic field have been calculated for center-doped GaAs/Al_xGa_{1-x}As quantum wells (QW's). The impurity states are calculated within a four-band effective-mass theory, in which the valence-band mixing as well as the mismatch of the band parameters and the dielectric constants between well and barrier materials have been taken into account. The g factors of the shallow acceptor $1s_{3/2}$ ground states and the $2p_{3/2}$ excited states are obtained for QW's with different well widths. The infrared optical transitions corresponding to the G , D , and C lines of acceptors in bulk GaAs have also been calculated versus magnetic fields up to 16 T for the case of acceptors confined in QW's.

I. INTRODUCTION

Acceptors confined in quantum-well (QW) structures have been investigated both experimentally¹⁻⁹ and theoretically.¹⁰⁻¹³ For instance, the well-width dependence of shallow acceptor energy levels has been measured experimentally^{1,6,10} and confirmed or predicted by theoretical calculations.^{10,12,13} Important experimental quantities are the acceptor binding energies and the $1s$ - $2s$ energy separations, measured by selective photoluminescence spectroscopy via free-to-bound transitions and two-hole transitions (THT), respectively. Since the acceptor binding energy is larger than the hole subband splitting, a proper treatment of the acceptor problem requires a four-band effective-mass Hamiltonian. In the absence of an external magnetic field, these calculations,¹⁰⁻¹³ which also take into account the mismatch of valence-band parameters and dielectric constants between well and barrier materials, are able to accurately reproduce experimental transition energies. The calculations in Refs. 11 and 12 also include continuum states in the basis set, which is important in order to obtain more accurate results both for the acceptor ground and excited states.

Because of the relative complexity of such calculations, the number of papers that deal with the presence of an external magnetic field is very limited. To our knowledge, the only work that considers the magnetic-field dependence of the acceptor ground states is Ref. 10. However, the predicted splitting due to a magnetic field in Ref. 10 is unrealistically large in comparison with experimental data,^{14,15} and thus calls for a theoretical confirmation.

In a recent paper,¹⁶ we have extended the theory by Fraizzoli and Pasquarello¹² to cover the case of an exter-

nal magnetic field. The advantage of this theory with respect to others is that it allows one to obtain acceptor ground states as well as excited states of any symmetry within the same framework. The calculated transition energies from the ground $1s_{3/2}(\Gamma_6)$ acceptor state to the $2s_{3/2}(\Gamma_6)$ excited state are in excellent agreement with experimental data.¹⁶

In this paper, we extend these calculations to treat transitions related to p -type excited states. We can thus calculate all possible infrared transitions between the $1s$ ground state and these excited states. For instance, the magnetic-field dependence of the infrared transitions denoted the G , D , and C lines in bulk GaAs, are calculated for the case of acceptors confined in QW's at magnetic fields up to 16 T. The validity of defining g values for different acceptor levels is discussed. In Sec. II, we present the theory that yields the energies and wave functions of acceptor states in QW's with an applied magnetic field perpendicular to the QW layers. The calculated g values are presented for well widths ranging from 50 to 200 Å. In Sec. III, we summarize the work presented.

II. ELECTRONIC STRUCTURE OF CONFINED ACCEPTORS IN QUANTUM WELLS

A. Theory

Considering a single QW, grown in the [001] direction, which we take as the quantization axis z , the acceptor Hamiltonian expressed in electron energy is given by a 4×4 matrix operator,¹²

$$H = -[H^{\text{kin}} + H^{\text{qw}} + H^c], \quad (1)$$

where H^{kin} represents the kinetic energy of the hole, H^{qw} the confinement potential due to the valence-band discontinuity, and H^c the potential of the acceptor impurity center and the image charges due to the mismatch of the dielectric constant. The kinetic-energy term H^{kin} , quadratic in $\mathbf{k} = -i\nabla + |e|\mathbf{A}/(\hbar c)$, describes the dispersion of the Γ_8 valence band with the external magnetic field $\mathbf{B} = \nabla \times \mathbf{A}$, and is given by the Luttinger-Kohn Hamiltonian¹⁷ in the axial approximation

$$H^{\text{kin}} = \begin{pmatrix} P+Q & L & M & 0 \\ L^+ & P-Q & 0 & M \\ M^+ & 0 & P-Q & -L \\ 0 & M^+ & -L^+ & P+Q \end{pmatrix} + 2\mu_B \kappa \mathbf{B} \cdot \mathbf{J} + q\mu_B (B_x J_x^3 + B_y J_y^3 + B_z J_z^3), \quad (2)$$

where

$$P = \frac{\gamma_1 \hbar^2}{2m_0} k^2, \quad (3a)$$

$$Q = \frac{\gamma_2 \hbar^2}{2m_0} (k_x^2 + k_y^2 - 2k_z^2), \quad (3b)$$

$$L = -i \frac{\sqrt{3} \gamma_3 \hbar^2}{2m_0} (k_x - ik_y) k_z, \quad (3c)$$

$$M = \frac{\sqrt{3} \hbar^2}{4m_0} (\gamma_2 + \gamma_3) (k_x - ik_y)^2, \quad (3d)$$

\mathbf{J} and \mathbf{B} are the hole angular momentum and the applied magnetic field, respectively, while μ_B is the Bohr magneton and m_0 is the free-electron mass. The $\gamma_1, \gamma_2, \gamma_3, \kappa$, and q are the Luttinger parameters describing the Γ_8 valence band. These parameters used for the well material and the barrier material, respectively, are given in Table I. The same Luttinger Hamiltonian as given above in the axial approximation has earlier been used to calculate the zero magnetic-field case¹² and the $1s_{3/2}(\Gamma_6)$ - $2s_{3/2}(\Gamma_6)$ energy separation in the presence of a magnetic field.¹⁶ A good agreement with experimental results was obtained. The QW potential represented by H^{qw} is a square-well potential of barrier height V and well width L_z . The Coulomb potential of a point charge in a system of three dielectrics separated by two infinite planes is contained in H^c . In order to satisfy the Maxwell boundary conditions, H^c must contain an infinite series of image charges.¹¹

We will restrict ourselves to an applied magnetic field

TABLE I. The Luttinger parameters.

	GaAs	AlAs
γ_1	6.85	3.45
γ_2	2.10	0.68
γ_3	2.90	1.29
ϵ	12.53	9.80
κ	1.20	0.12
q	0.04	0.03

along the z direction in the following discussion. Therefore, the vector potential \mathbf{A} is defined as

$$\mathbf{A} = \frac{1}{2} \mathbf{B} \times \mathbf{r} = \frac{1}{2} (-yB, xB, 0), \quad (4)$$

where B is the magnetic-field strength along the z direction. The twofold degeneracy of the acceptor levels in the zero magnetic-field case is now lifted in the presence of a magnetic field along the z direction, due to the breakdown of the time-reversal symmetry.

The acceptor wave functions can be written as a four-component envelope function $F^m(\rho, \theta, z) = [F^{m,s}] = [F^{m,3/2}, F^{m,1/2}, F^{m,-1/2}, F^{m,-3/2}]$, where m is the hole angular momentum and is a good quantum number. The notations $(m, +)$ and $(m, -)$, defined in Ref. 11, will be used in the following, and represent even and odd symmetry, respectively. Both $(m, +)$ and $(m, -)$ represent doublets with angular momentum $+m$ and $-m$, which are degenerate in the absence of an external magnetic field. In the presence of an external magnetic field, such a degeneracy will be lifted. When the Hamiltonian given in (1) acts on this four-component function F^m ,

$$HF^m = EF^m, \quad (5)$$

the energy positions of the shallow acceptor states and corresponding wave functions are derived. The s component of an acceptor envelope function of definite angular momentum m can be expanded into a basis set of functions, which are separable in the coordinates ρ and z :

$$F^{m,s}(\rho, \theta, z) = e^{i(m-s)\theta} f^{m,s}(\rho, z) = e^{i(m-s)\theta} \sum_n R_n^{m,s}(\rho) g_n^s(z). \quad (6)$$

The function g_n^s is chosen to be the s component of the four-component envelope function g_n , which describes a QW subband state at $\mathbf{k}_{\parallel} = 0$. The envelope function g_n is a solution of the Hamiltonian $H^{\text{kin}} + H^{\text{qw}}$ at zero magnetic field. It has earlier been shown¹² that it is necessary to include not only the discrete states but also the continuum states of the impurity-free QW in the basis set of the functions g_n in order to achieve numerical convergence for the binding energies of the acceptor ground states. The continuum states are taken into account by introducing sufficiently separated infinite barriers, which transform all the continuum states into discrete states.

The radial functions $R_n^{m,s}(\rho)$ in Eq. (6) are developed in an expansion of functions with ρ :

$$R_n^{m,s}(\rho) = \rho^{|m-s|} \sum_l A_{nl}^{m,s} e^{-\alpha_l \rho}, \quad (7)$$

where the exponents α_l are chosen in a geometrical series and cover the relevant physical region. The coefficients $A_{nl}^{m,s}$ are taken as variational parameters. The eigenvalue problem can be turned into a linear problem for the parameters $A_{nl}^{m,s}$. For a given symmetry, the lowest state as well as the excited ones are calculated at the same time. According to the treatment of the impurity potential by Fraizzoli and Pasquarello,¹² the matrix elements related to H^c can be calculated with a one-dimensional numerical integral with the present basis set of wave functions. In

this way, a large number of basis functions, up to 50 for the functions g_n and 12 exponential functions in Eq. (6), are included in our calculations. The convergence of the calculations is quite fast as long as the magnetic length $L_b = \sqrt{\hbar/eB}$ is not significantly smaller than the in-plane orbital length of the acceptor states. The number of basis functions used can be different for different symmetry states. Generally, for more localized states, a larger number of basis functions is needed.

B. Results and discussions

The results presented below are applicable for acceptors confined in center-doped GaAs/Al_xGa_{1-x}As QW's. Before the calculated results are presented, a few points should be emphasized. First, there are three terms in the kinetic-energy part of the Hamiltonian [Eq. (2)], which depend on the magnetic field B . The first term in Eq. (2) includes both a linear and a quadratic magnetic-field dependence. The linear magnetic-field dependence resulting from the first term is dominant and has a different sign with respect to the last two terms in Eq. (2) for the ground acceptor states. Accordingly, the total-energy splitting in the presence of a magnetic field is the result of partially compensating contributions. This has the consequence that an increasing value for the Luttinger parameter κ gives rise to a decreasing splitting of the acceptor states in the presence of an external magnetic field, as has been shown in our previous paper (see Fig. 2 of Ref. 16). Second, the last term in Eq. (2) has a non-negligible effect on the splitting of acceptor levels with an applied magnetic field. Figure 1 shows the binding energy of the heavy-hole $1s$ acceptor ground state calculated with and without inclusion of the last term in Eq. (2), with the q parameter as given in Table I. The result shown in Fig. 1 clearly demonstrates the importance of this term. Third, the splitting of the acceptor levels in the presence of a magnetic field strongly depends on the

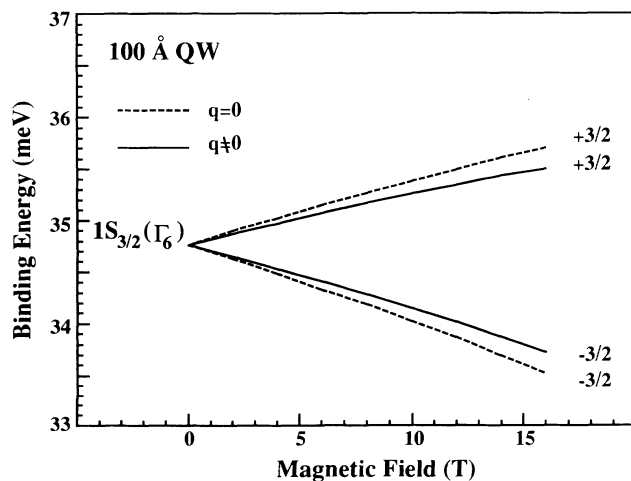


FIG. 1. The splitting of the $1s$ heavy-hole acceptor states vs an applied magnetic field, calculated with (solid line) and without (dashed lined) including the last term of Eq. (2). The values for the q parameter are given in Table I.

Luttinger parameter κ . In our previous calculations,¹⁶ we have confirmed that the Luttinger parameter κ in bulk GaAs is close to 1.2 by comparing our calculated and experimental results on the $1s$ - $2s$ transition energy. In the following numerical calculations, the Luttinger parameters given in Table I are used. The parameters for the Al_xGa_{1-x}As alloy are obtained by a linear interpolation between the GaAs and the AlAs parameters. An offset ratio between the conduction and the valence band of 65 to 35 has been assumed and the valence-band discontinuity for the Al_xGa_{1-x}As alloy is accordingly taken as $\Delta E_v = 0.35 \times 1247x$ meV.

Figures 2 and 3 show the magnetic-field dependencies of the lowest energy levels for on-center acceptors in 100-Å-wide GaAs/Al_{0.3}Ga_{0.7}As QW's for a magnetic field up to 16 T. The acceptor energies are given with respect to the bottom of the first heavy-hole subband, which is the lowest hole level in an impurity-free QW. Figure 2 shows the even symmetric acceptor states. Solid, dashed, and dotted-dashed curves correspond to states with $(\frac{3}{2}, +)$, $(\frac{1}{2}, +)$, and $(\frac{5}{2}, +)$ symmetry, respectively. The fourfold degenerate acceptor ground state in bulk, $1s_{3/2}(\Gamma_8)$, is split into two twofold degenerate states, $1s_{3/2}(\Gamma_6)$ and $1s_{3/2}(\Gamma_7)$, when the acceptors are located at the center of the QW, at zero magnetic field. The $1s_{3/2}(\Gamma_6)$ and $1s_{3/2}(\Gamma_7)$ states are related to the heavy-hole ground state of $(\frac{3}{2}, +)$ symmetry and the light-hole ground state of $(\frac{1}{2}, +)$ symmetry, respectively. When a magnetic field is applied along the z direction, the degeneracy is further lifted. This Zeeman splitting is larger for the heavy-hole related $1s_{3/2}(\Gamma_6)$ ground states

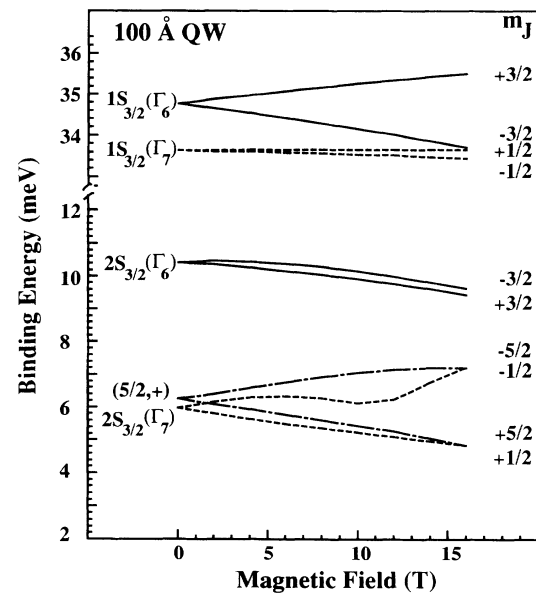


FIG. 2. The magnetic-field dependence of the binding energy of the even-parity acceptor states for an on-center impurity in a 100-Å-wide GaAs/Al_{0.3}Ga_{0.7}As QW. Solid, dashed, and dotted-dashed curves are used for states of the $(\frac{3}{2}, +)$, $(\frac{1}{2}, +)$, and $(\frac{5}{2}, +)$ symmetry, respectively. The binding energies are given with respect to the bottom of the first heavy-hole subband.

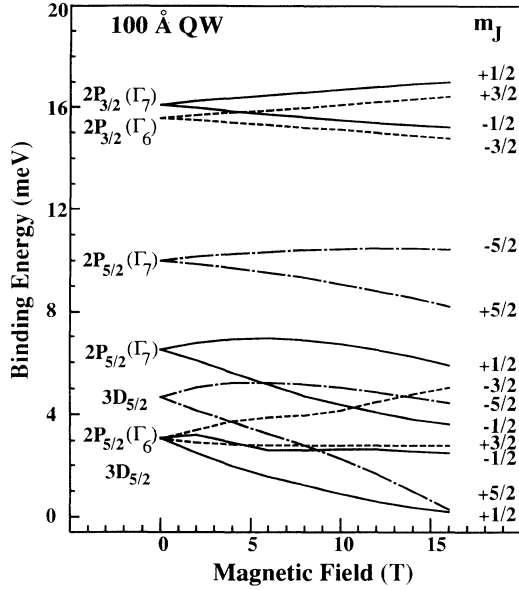


FIG. 3. The magnetic-field dependence of the binding energy of the odd-parity acceptor states for an on-center impurity in a 100-Å-wide GaAs/Al_{0.3}Ga_{0.7}As QW. Solid, dashed, and dotted-dashed curves are used for states of the $(\frac{1}{2}, -)$, $(\frac{3}{2}, -)$, and $(\frac{5}{2}, -)$ symmetry, respectively. The binding energies are given with respect to the bottom of the first heavy-hole subband.

than for the light-hole related $1s_{3/2}(\Gamma_7)$ ground states as illustrated in Fig. 2. The corresponding Zeeman splitting for the excited $2s$ heavy-hole states is much smaller than for the $1s$ heavy-hole ground states, while the opposite is true for light-hole acceptor states.

Figure 3 shows the binding energies of the odd symmetric acceptor states. Solid, dashed, and dotted-dashed curves illustrate the magnetic-field dependence of states with $(\frac{1}{2}, -)$, $(\frac{3}{2}, -)$, and $(\frac{5}{2}, -)$ symmetry, respectively. The bulk states $2p_{3/2}$ and $2p_{5/2}$ split in a QW into doublet states, which are further split in the presence of a magnetic field as illustrated in Fig. 3.

The splitting of the even and odd symmetric acceptor levels is generally not linearly dependent on the magnetic field, as can be seen in Figs. 2 and 3, especially for the excited states. In the following, we will discuss some physical quantities, which can be directly compared with experimental data.

In infrared absorption measurements, transitions between the $1s$ ground state and the different excited s -like states are forbidden. However, the $1s$ - $2s$ energy separation can be deduced from selective photoluminescence (PL) and resonant Raman measurements.⁶ Figure 4 shows the energy separations between the $1s_{3/2}(\Gamma_6)$ ground state and the $2s_{3/2}(\Gamma_6)$ excited state together with the lowest level of the $(\frac{5}{2}, +)$ symmetric states. On the other hand, many transitions from the $1s$ ground state to different odd symmetric states can be measured by infrared measurements. For instance, the transitions denoted G , D , and C lines in bulk GaAs material correspond to the transitions from the $1s_{3/2}(\Gamma_6)$ and the $1s_{3/2}(\Gamma_7)$ ground states to the $2p_{3/2}$ and the $2p_{5/2}$ excited

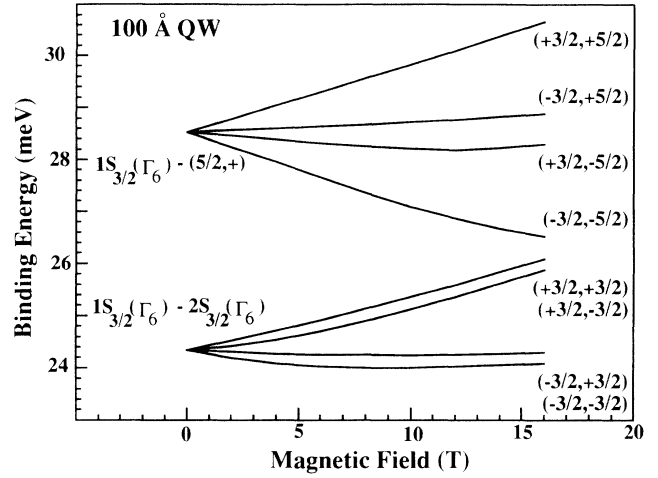


FIG. 4. The magnetic-field dependence of transitions from the $1s$ heavy-hole acceptor state to the excited s -like acceptor states in a 100-Å-wide GaAs/Al_{0.3}Ga_{0.7}As QW.

states. Figure 5 shows the magnetic-field dependence of the G -, D -, and C -line transitions for acceptors confined in 100-Å-wide QW's. The σ (in the xy plane) and π (along the z direction) polarization are indicated by the solid and the dashed lines, respectively.

The $1s_{3/2}(\Gamma_6)$ - $2s_{3/2}(\Gamma_6)$ acceptor transition energies have been measured as a function of magnetic field by means of the resonant Raman-scattering technique. The predicted transition energies derived from our calculations are in good agreement with the experimental results available.¹⁶ For the case of the G , D , and C transitions shown in Fig. 5, there are, to our knowledge, no corresponding experimental results available so far.

C. g factor of acceptors in QW's

The g factor is a parameter to describe the linear splitting of acceptor states with an applied magnetic field. The splitting of the $\pm|J_z|$ states can be written as

$$\Delta E_m = \mu_B g_{J_z} B [|J_z| - (-|J_z|)] = 2\mu_B g_{J_z} |J_z| B, \quad (8a)$$

or alternatively

$$\Delta E_m = \mu_B g_{J_z} B, \quad (8b)$$

where J_z is the magnetic angular momentum along the direction of the magnetic field and g_{J_z} is a g value related to the angular momentum J_z . Obviously, the definitions used in Eqs. (8a) and (8b) differ by a factor $2|J_z|$, which means that for the $|\pm\frac{3}{2}\rangle$ state, the g values given by Eqs. (8a) and (8b) differ by a factor of 3, while for the $|\pm\frac{1}{2}\rangle$ states, the two definitions are identical. We will use the definition in Eq. (8b) in the following discussion. It is important to note that the system to be discussed is the symmetric center-doped QW, i.e., the $|\pm m\rangle$ states are degenerate without an external magnetic field. If the symmetry is low enough to lift such a degeneracy at zero magnetic field, the definition Eq. (8) is not valid any more. From the definition given in Eq. (8b), together

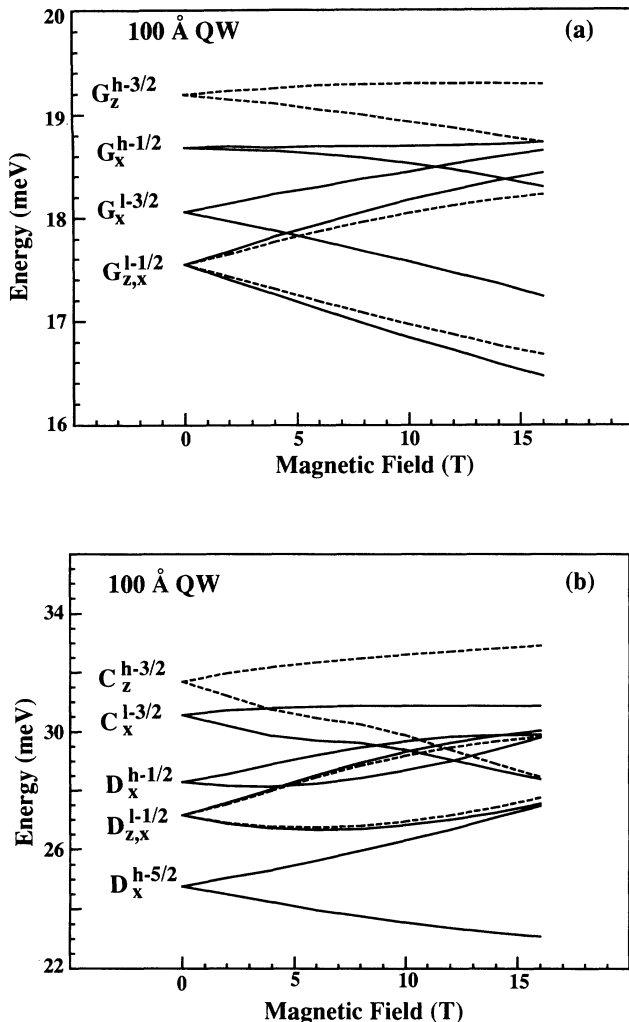


FIG. 5. The magnetic-field dependence of the infrared transitions corresponding to the (a) G line, (b) D and C lines for acceptors confined in a 100-Å-wide GaAs/Al_{0.3}Ga_{0.7}As QW. The σ (in xy plane) and π (along z direction) polarization transitions are indicated by the solid and the dashed lines. The notations used refer to Ref. 12.

with the magnetic-field dependence of acceptor energy levels calculated in the above section, the g values can be deduced.

In Fig. 6, the g values of the confined acceptor $1s_{3/2}$ ground states and $2p_{3/2}$ states are plotted for different well widths. The g values are deduced at 6 T for all states shown in Fig. 6. As mentioned earlier, the splitting of the acceptor levels is generally not linear with the applied magnetic field as illustrated in Figs. 2 and 3. This raises the question of how the g values vary with the applied magnetic field. If the g value strongly depends on the applied magnetic field, it is meaningless to define a constant g factor. Therefore, we have calculated g values for magnetic fields from 1 to 16 T. The results show that the g -value variation is less than 2% for the $1s_{3/2}(\Gamma_6)$ and $2p_{3/2}(\Gamma_6)$ states, less than 6% for the $1s_{3/2}(\Gamma_7)$ state, and less than 15% for the $2p_{3/2}(\Gamma_7)$ state with the magnetic field up to 16 T. Accordingly, we can conclude that it is

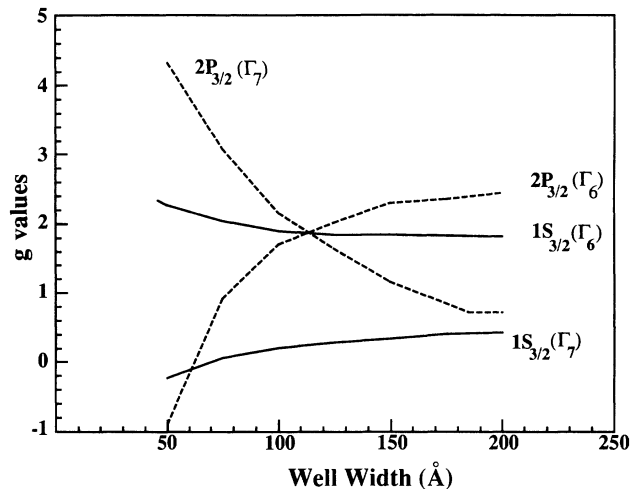


FIG. 6. The g values of the $1s_{3/2}$ and $2p_{3/2}$ acceptor states calculated vs the well width.

still a satisfactory approximation to use a constant g factor to describe the splitting for the ground $1s$ acceptor states, and also for the $2p_{3/2}(\Gamma_6)$ states. For the $2p_{3/2}(\Gamma_7)$ state, the variation with field is too large to define a constant g factor.

The results in Fig. 6 show that the g values of the $1s_{3/2}(\Gamma_6)$ and the $1s_{3/2}(\Gamma_7)$ acceptor states have a different behavior with varying well width. The g value of the $1s_{3/2}(\Gamma_6)$ acceptor states increases with decreasing well width, while the g value of the $1s_{3/2}(\Gamma_7)$ acceptor states decreases. Furthermore, the g values both for the $1s_{3/2}(\Gamma_6)$ and $1s_{3/2}(\Gamma_7)$ states vary less with QW width than the $2p_{3/2}$ states because the $2p_{3/2}$ states are more extended than the $1s_{3/2}$ states and feel the change in well width much more than the $1s_{3/2}$ states. Our calculations show that the g values vary from 1.81 to 2.27 for the $1s_{3/2}(\Gamma_6)$ state and from 0.43 to -0.23 for the $1s_{3/2}(\Gamma_7)$ state when the well width decreases from 200 to 50 Å. It should be pointed out that it has earlier been concluded that the splitting of the acceptor states due to a magnetic field (g values) in QW's is practically identical to that of the bulk acceptor for the $1s_{3/2}$ ground states.

The g values for our calculations are in excellent agreement with the experimental results from Ref. 15. There is no adjustable parameter in these calculations. The Luttinger parameters are the only input parameters. Therefore, the accuracy of the calculated results depends solely on the accuracy of these parameters.¹⁰

As mentioned earlier, the splitting of the acceptor levels is very sensitive to the κ parameter, in particular the energy separation corresponding to the $1s$ - $2s$ acceptor states but also of the transitions corresponding to the G , D , and C lines. Therefore, by combining our calculations with experimental data on the magnetic-field dependence of the transition-energy separations, the κ parameter for bulk material can be accurately determined, i.e., an independent approach to obtain the important Luttinger parameter κ . This method should be applicable to other bulk alloy materials, where it is difficult to accurately es-

timate the κ value due to a poor resolution of the exciton splitting with an applied magnetic field.

III. SUMMARY

A four-band effective-mass model has been used to calculate the acceptor states in QW's in the presence of an applied magnetic field. The magnetic field is applied parallel to the growth direction of the QW structures. The valence-band mixing, and the mismatch of the valence-band Luttinger parameter and the dielectric constant, have been taken into account in these calculations.

We have calculated the magnetic-field dependence of the acceptor energy levels in QW's. The infrared transitions corresponding to the G , D , and C lines in bulk are

calculated for shallow acceptors confined in a QW with different magnetic fields both for the σ (in xy plane) and π (along z direction) polarizations. The transitions between the $1s$ heavy-hole acceptor state and the excited s -like states as a function of magnetic field have been calculated. Our calculated results show an excellent agreement with such experimental data¹⁶ on the $1s$ - $2s$ energy separations determined by selective PL measurements via the THT satellites.

Furthermore, the g values of the acceptors confined in QW's have been calculated for different well widths. The variation of the g values is found to be less than 2% for the $1s_{3/2}(\Gamma_6)$ and $2p_{3/2}(\Gamma_6)$ states, and less than 6% for the $1s_{3/2}(\Gamma_7)$ state when the magnetic field is varied from 0 up to 16 T.

¹R. C. Miller, A. C. Gossard, W. T. Tsang, and O. Munteanu, Phys. Rev. B **25**, 3871 (1982).

²X. Liu, A. Petrou, B. D. McCombe, J. Ralston, and G. Wicks, Phys. Rev. B **38**, 8522 (1988).

³P. O. Holtz, M. Sundaram, R. Simes, J. L. Merz, A. C. Gossard, and J. H. English, Phys. Rev. B **39**, 13 293 (1989).

⁴P. O. Holtz, M. Sundaram, K. Doughty, J. L. Merz, and A. C. Gossard, Phys. Rev. B **40**, 12 338 (1989).

⁵P. O. Holtz, Q. X. Zhao, B. Monemar, M. Sundaram, J. L. Merz, and A. C. Gossard, Phys. Rev. B **47**, 15 675 (1993).

⁶P. O. Holtz, Q. X. Zhao, A. C. Ferreira, B. Monemar, M. Sundaram, J. L. Merz, and A. C. Gossard, Phys. Rev. B **48**, 8872 (1993).

⁷A. A. Reeder, B. D. McCombe, F. A. Chambers, and G. P. Devane, Phys. Rev. B **38**, 4318 (1988).

⁸B. V. Shanabrook, J. Comas, T. A. Perry, and R. Merlin, Phys. Rev. B **29**, 7096 (1984).

⁹D. Gammon, R. Merlin, W. T. Masselink, and H. Morkoc, Phys. Rev. B **33**, 2919 (1986).

¹⁰W. T. Masselink, Y.-C. Chang, and H. Morkoc, Phys. Rev. B **28**, 7373 (1983); **32**, 5190 (1985).

¹¹A. Pasquarello, L. C. Andreani, and R. Buczko, Phys. Rev. B **40**, 5602 (1989).

¹²S. Fraizzoli and A. Pasquarello, Phys. Rev. B **42**, 5349 (1990); **44**, 1118 (1991).

¹³G. T. Einevoll and Y.-C. Chang, Phys. Rev. B **41**, 1447 (1990).

¹⁴D. N. Mirlin and A. A. Sirenko, Fiz. Tverd. Tela (St. Petersburg) **34**, 205 (1992) [Sov. Phys. Solid State **34**, 108 (1992)].

¹⁵V. F. Sapega, M. Cardona, K. Ploog, E. L. Ivchenko, and D. N. Mirlin, Phys. Rev. B **45**, 4320 (1992).

¹⁶Q. X. Zhao, P. O. Holtz, A. Pasquarello, B. Monemar, A. C. Ferreira, M. Sundaram, J. L. Merz, and A. C. Gossard, Phys. Rev. B **49**, 10 794 (1994).

¹⁷J. M. Luttinger, Phys. Rev. **102**, B1030 (1956).